NASA CONTRACTOR
REPORT

NASA CR-1834

RADIATION EFFECTS DESIGN HANDBOOK

Section 4. Transistors

by J. E. Drennan and D. J. Hamman

Prepared by
RADIATION EFFECTS INFORMATION CENTER
BATTELLE MEMORIAL INSTITUTE
Columbus, Ohio 43201
for

NATIONAL AERONAUTICS AND SPACE ADMINISTRATION • WASHINGTON, D. C. • AUGUST 1971

1. Report No.	2. Government Accession No.	3. Recipient's Catalog No.
NASA CR-1834		

4. Title and Subtitle	5. Report Date
RADIATION EFFECTS DESIGN HANDBOOK SECTION 4. TRANSISTORS	August 1971
	6. Performing Organization Code
7. Author(s)	8. Performing Organization Report No.
J. E. Drennan and D. J. Hamman	
	10. Work Unit No.
9. Performing Organization Name and Address	11. Contract or Grant No.
RADIATION EFFECTS INFORMATION CENTER Battelle Memorial Institute Columbus Laboratories Columbus, Ohio 43201	NASW-1568
	13. Type of Report and Period Covered
12. Sponsoring Agency Name and Address	Contractor Report
National Aeronautics and Space Administration Washington, D. C. 20546	14. Sponsoring Agency Code

15. Supplementary Notes

16. Abstract

This document contains summarized information relating to steady-state radiation effects on transistors. The radiations considered include neutrons, protons, electrons, and electromagnetic. The information is useful to the design engineer for estimating the effects of radiation on transistors.

17. Key Words (Suggested by Author(s))	18. Distribution Statement
Radiation effects, Transistors, Semiconductors, Bipolar Transistor, Unijunction Transistors, JFETS, MOSFET	Unclassified-Unlimited

19. Security Classif. (of this report)	20. Security Classif. (of this page)	21. No. of Pages	22. Price*
Unclassified	Unclassified	38	$3.00

*For sale by the National Technical Information Service, Springfield, Virginia 22151

ACKNOWLEDGMENTS

The Radiation Effects Information Center owes thanks to several individuals for their comments and suggestions during the preparation of this document. The effort was monitored and funded by the Space Vehicles Division and the Power and Electric Propulsion Division of the Office of Advanced Research and Technology, NASA Headquarters, Washington, D. C., and the AEC-NASA Space Nuclear Propulsion Office, Germantown, Maryland. Also, we are indebted to the following for their technical review and valuable comments on this section:

Mr. R. A. Breckenridge, NASA-Langley Research Center

Mr. F. Gordon, Jr., NASA-Goddard Space Flight Center

Dr. A. G. Holmes-Siedle, RCA

Mr. S. Manson, NASA Hq.

Mr. D. Miller, NASA-Space Nuclear Systems Office

Mr. A. Reetz, Jr., NASA Hq.

Dr. A. G. Stanley, Massachusetts Institute of Technology

Mr. W. T. White, NASA-Marshall Space Flight Center

PREFACE

This is the fourth section of a Radiation Effects Design Handbook designed to aid engineers in the design of equipment for operation in the radiation environments to be found in space, be they natural or artificial. This Handbook will provide the general background and information necessary to enable designers to choose suitable types of materials or classes of devices.

Other sections of the Handbook discuss such subjects as solar cells, thermal-control coatings, structural metals, interactions of radiation, electrical insulating materials, and capacitors.

SECTION 4. TRANSISTORS

INTRODUCTION

This portion of the Handbook presents information about the effects of radiation on bipolar transistors, unijunction transistors, and field-effect transistors (FET's). Data presentation is graphic wherever possible, consisting of envelopes that enclose the data points for a particular parameter. Where possible, representative sets of data points also are plotted.

The reader is cautioned that the intent of the presentation in the following paragraphs is to give a broad picture of radiation effects on general classes of transistors. If the intended application requires a radiation fluence greater than that for which information is presented, further information for the specific device of interest should be sought.

BIPOLAR TRANSISTORS

The two structures of bipolar transistors are shown schematically in Figure 1. Both silicon and germanium bipolar transistors are available in both of these structures.

The radiation effects of greatest significance* in bipolar transistors are the displacements in the semiconductor crystal lattice caused by the incident radiation. Radiation particles lose energy primarily by elastic collisions with the semiconductor atoms and, depending on type and energy, may cause large disordered clusters to be formed within the material. Electromagnetic radiation, in contrast, loses energy by creating Compton electrons which then may cause lattice displacements. Since electrons have such a small mass, however, they primarily cause Frenkel defects (vacancy-interstitial pairs) rather than clusters of defects. Lattice damage due to electromagnetic radiation is usually of secondary importance unless a large dose (greater than 10^5 rads) is absorbed by the material.

Lattice damage degrades the electrical characteristics of bipolar transistors by increasing the number of trapping, scattering, and recombination centers as follows:

*At high radiation intensities such as may be experienced in a pulse environment, other effects may be dominant.

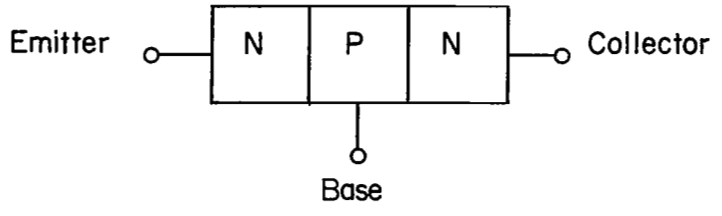

a. NPN Transistor Structural Diagram

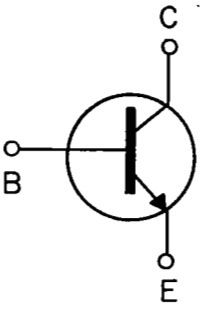

b. NPN Transistor Schematic Symbol

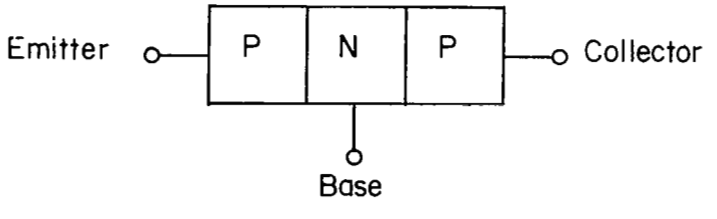

c. PNP Transistor Structural Diagram

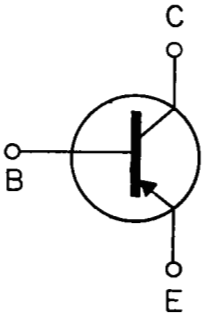

d. PNP Transistor Schematic Symbol

FIGURE 1. STRUCTURAL DIAGRAMS AND SCHEMATIC SYMBOLS FOR BIPOLAR TRANSISTORS

(1) The trapping centers remove carriers from the conduction process. N- and P-type silicon gradually changes toward intrinsic material with increased radiation exposure. N-type germanium irradiated with neutrons or protons is converted to P-type. The conductivity of P-type germanium increases or decreases monotonically with bombardment, approaching the same limiting value that the converted N-type reaches.

(2) The additional scattering centers reduce the mean-free path of the free carriers. Since the mobility is directly proportional to the mean-free path, radiation exposure reduces the mobility of charge carriers.

(3) The recombination centers decrease the minority-carrier lifetime according to the relationship:

$$\frac{1}{\tau_\Phi} = \frac{1}{\tau_o} + K_\tau \Phi \quad . \tag{1}$$

(See Introduction to Section 1., Semiconductor Devices.)

The dominant radiation effect for bipolar transistors is the degradation of the forward current gain (h_{FE}, β) resulting from the radiation-induced decrease of minority-carrier lifetime, τ. β is defined by:

$$\beta = \frac{2D}{W^2} \tau \quad , \tag{2}$$

where

D = diffusion constant

W = effective base width.

Simple theory predicts a linear change in reciprocal low frequency gain, $1/\beta$, with fluence as shown by the relation:

$$\left(\frac{1}{\beta_\Phi} - \frac{1}{\beta_o}\right) = \Delta\ (1/\beta) = \left(\frac{1.22}{2\pi}\right) \left(\frac{K_\tau}{f_{\alpha co}}\right) \Phi \quad , \tag{3}$$

where

β_Φ = common-emitter low frequency gain at some value of fluence

β_o = preirradiation common-emitter low frequency gain

Φ = radiation fluence (particle/cm^2)

K_τ = minority-carrier-lifetime damage constant for the material and type of radiation

$f_{\alpha co} = f\left(\frac{D}{W^2}\right)$ = alpha cutoff frequency defined as the frequency at which the magnitude of the common-base small-signal current gain is reduced to 70.7 percent of its initial value.

At the low fluence, $1/\beta$ does not depend linearly on fluence, an effect attributed to surface damage. A power-law fit of data obtained at low $\Delta(1/\beta)$, is proportional to $(\Phi)^n$, where $0 < n < 1$. Hence, the general expression for silicon-transistor low-frequency current-gain degradation for fluence levels sufficiently low that conductivity changes are neglible is

$$\Delta(1/\beta) = K_b \Phi + K_s (\Phi)^n; \Phi < (\Phi)_{sat}$$

$$\Delta(1/\beta) = [\Delta(1/\beta)]_{sat}; \Phi = (\Phi)_{sat}$$

$$\Delta(1/\beta) = K_b [\Phi - (\Phi)_{sat}] + [\Delta(1/\beta)]_{sat}; \Phi > (\Phi)_{sat} . \quad (4)$$

where

K_b = bulk-damage constant = $\frac{(1.22)}{2\pi} \frac{(K_\tau)}{f_{\alpha co}}$ (cm^2/particle)

K_s = surface-damage constant (cm^2/particle)

n = a positive exponent greater than 0 but less than 1

$[\Delta(1/\beta)]_{sat}$ = the saturated value of the surface-damage curve

$(\Phi)_{sat}$ = the fluence level at which saturation of the surface-damage curve occurs (particles/cm^2).

This relation provides the basic tool for estimating the degradation of transistor-current gain caused by radiation by means of the quantities K_b, K_s, n, and the measurable parameters of the device, β_o and $f_{\alpha co}$. The

greatest uncertainties in using this relation are the values of the damage constants, K_b and K_s, and the exponent, n. This is because the values for a given transistor may vary widely with current density and impurity variations of the base material. The values will also depend upon the type and energy of the bombarding particle.

At the present time, experimental values of K_b, K_T, K_s, and n are extremely limited. Further, it must be recognized that the radiation-induced change of the bipolar transistor current gain also will depend on the type of semiconductor material, type of impurity (N or P), resistivity, fabrication technique, device structure, etc., as well as injection level, temperature, electrical bias conditions, energy spectrum of the incident radiation, and the time since the radiation exposure. Accordingly, the available theory cannot be applied effectively for detailed predictions of expected radiation effects for a specific application. However, the theory does provide a basis for presenting generalized information useful in guiding decisions about application of transistors in radiation environments. Thus, one can estimate whether or not a radiation effects problem is likely to exist for a specific application and if such is the case, then steps can be taken to obtain the necessary specific information.

The theory has been applied to approximate K_b using available experimental values of $\Delta(1/\beta)$ and Φ in the relation:

$$K_b = \frac{\Delta(1/\beta)}{\Phi} \quad . \tag{5}$$

This approximation is larger than the theoretical value of K_b by the amount $[\Delta(1/\beta)]_{sat}/\Phi$. Available data generally do not provide an experimental value of $[\Delta(1/\beta)]_{sat}$, so only the approximate value of K_b can be calculated.

The calculated value of K_b is used to estimate the value of fluence, Φ_{50}, for which the theory predicts that the gain would be 50 percent of its initial value:

$$\Phi_{50} \cong \frac{1}{K_b \beta_o} \quad . \tag{6}$$

The radiation-induced degradation of the beta ratio, β_n, is shown by theory to follow:

$$\beta_n = \beta_\Phi/\beta_o = \frac{\Phi_{50}}{\Phi_{50} + \Phi_{\beta_n}} \quad , \tag{7}$$

where Φ_{β_n} is the fluence for which a beta ratio value of β_n is predicted by the theory.

The available data for bipolar transistors have been grouped according to the application for which each transistor was designed. The five application groups used are: audio and general purpose, high frequency, low-level switching, high-level switching, and power. Equations (5) and (6) were used to estimate values of K_b and Φ_{50} for each experimental data point for which meaningful degradation was observed. The maximum and minimum values of Φ_{50} for each application group were used with Equation (7) to generate an envelope of potentially significant radiation damage that includes the available data.

Figures 2 through 21 present plots* of the radiation-effects envelopes obtained for each application for each of the radiation environments: neutron, proton, electron, and electromagnetic. Points for selected sets of bipolar transistor data are included on these plots. Table 1 lists the maximum, minimum, and median K_b values determined for each application-environment category and the number of sets of data used to establish these values.

In applying the plots, one should determine if the specific environment of interest lies: (1) outside the envelope in the low-fluence region, (2) within the envelope, or (3) outside the envelope in the high-fluence region. The interpretation of these three alternatives is that for Case 1 there probably is no radiation effects problem; Case 2 signifies a potential problem with radiation effects indicating that additional information should be obtained; and Case 3 indicates a virtual certainty of severe radiation effects implying a high probability that bipolar transistors will not perform satisfactorily in this specific application.

*The low frequency common emitter current gain ratio, $\beta_n = \beta_\Phi / \beta_o = \beta_F / \beta_o$, is plotted versus fluence. The number of data sets listed on the figures is the total number of (β_n, Φ) points available from which those plotted were selected as representative.

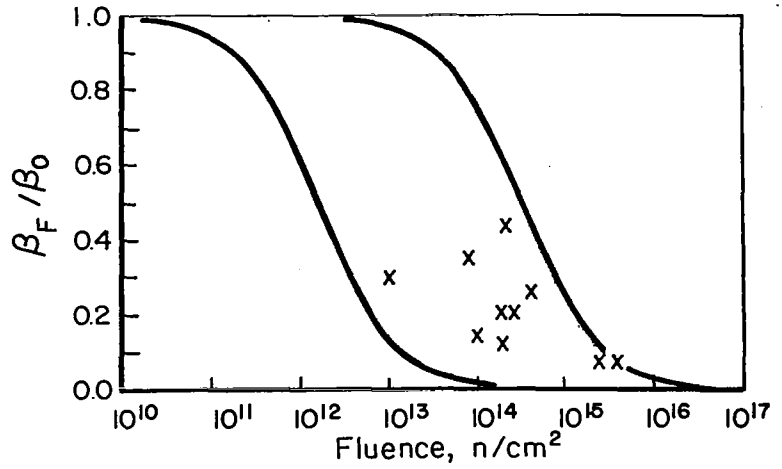

FIGURE 2. NEUTRON ENVIRONMENT AUDIO AND GENERAL PURPOSE APPLICATIONS, BIPOLAR TRANSISTOR BETA RATIO VERSUS FLUENCE

21 sets of data

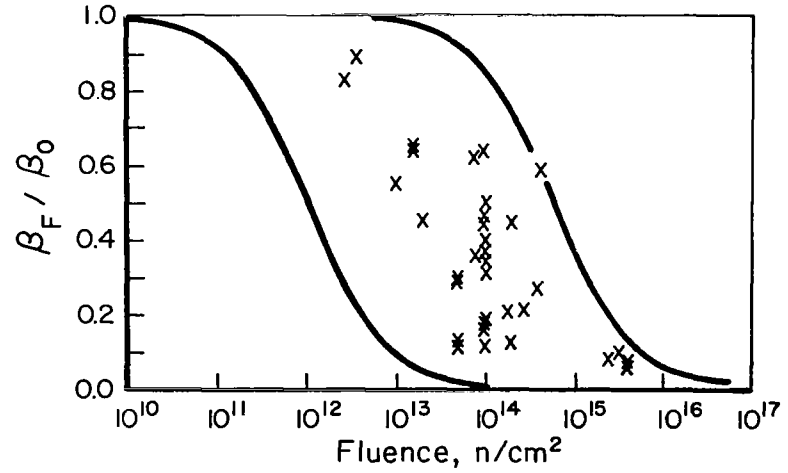

FIGURE 3. NEUTRON ENVIRONMENT HIGH-FREQUENCY APPLICATIONS, BIPOLAR TRANSISTOR BETA RATIO VERSUS FLUENCE

131 sets of data

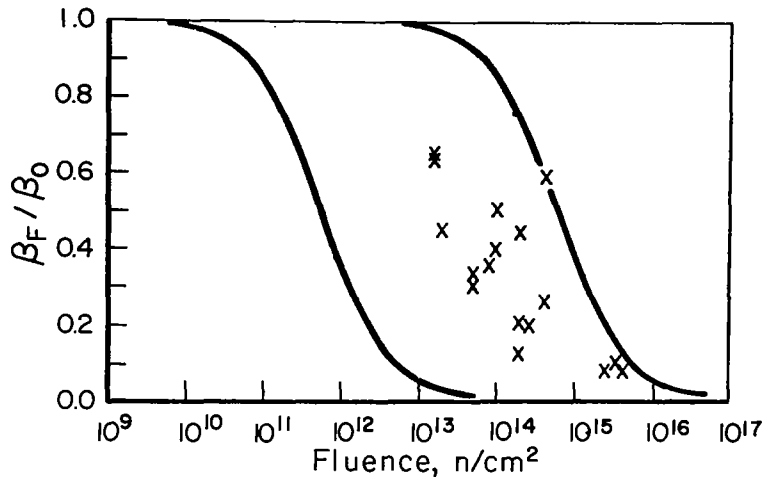

FIGURE 4. NEUTRON ENVIRONMENT LOW-LEVEL-SWITCHING APPLICATIONS, BIPOLAR TRANSISTOR BETA RATIO VERSUS FLUENCE

62 sets of data

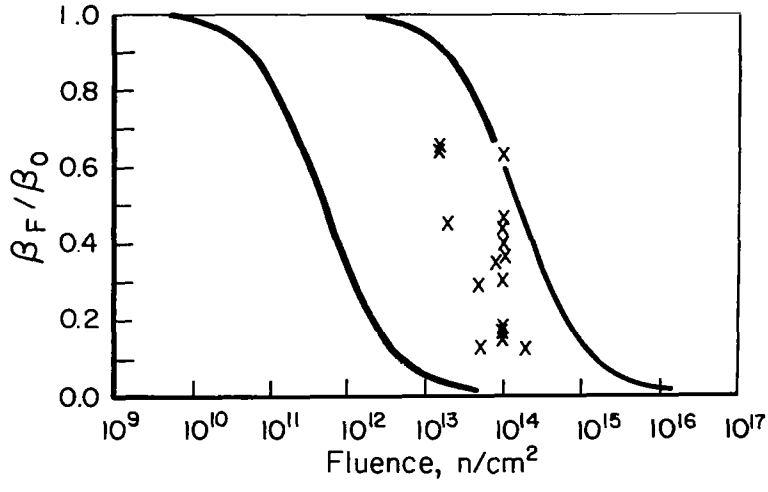

FIGURE 5. NEUTRON ENVIRONMENT HIGH-LEVEL-SWITCHING APPLICATIONS, BIPOLAR TRANSISTOR BETA RATIO VERSUS FLUENCE

73 sets of data

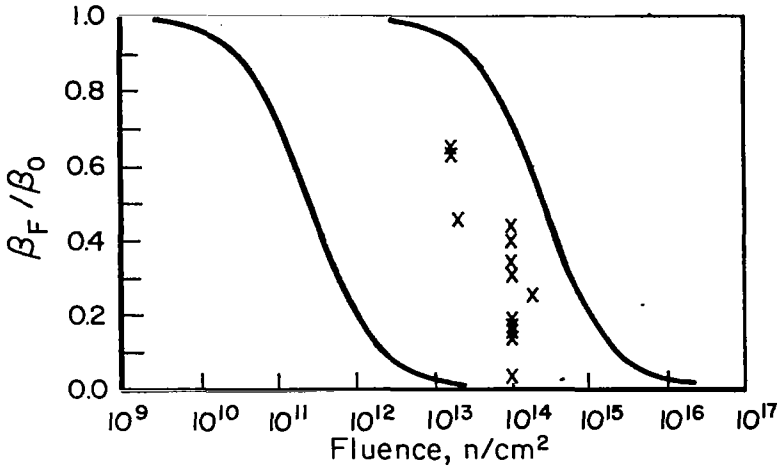

FIGURE 6. NEUTRON ENVIRONMENT POWER APPLICATIONS, BIPOLAR TRANSISTOR BETA RATIO VERSUS FLUENCE

72 sets of data

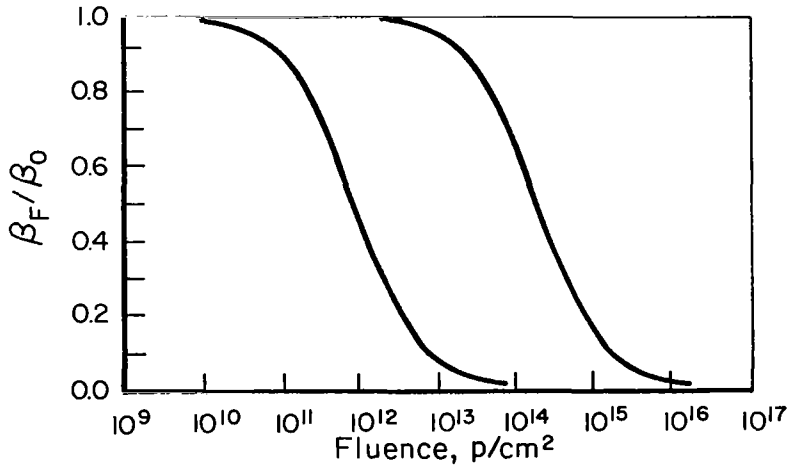

FIGURE 7. PROTON ENVIRONMENT AUDIO AND GENERAL PURPOSE APPLICATIONS, BIPOLAR TRANSISTOR BETA RATIO VERSUS FLUENCE

3 sets of data

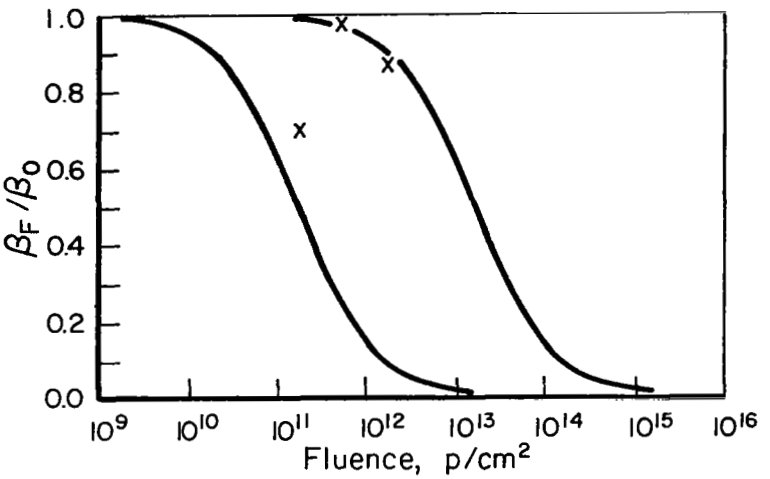

FIGURE 8. PROTON ENVIRONMENT HIGH-FREQUENCY APPLICATIONS, BIPOLAR TRANSISTOR BETA RATIO VERSUS FLUENCE

29 sets of data

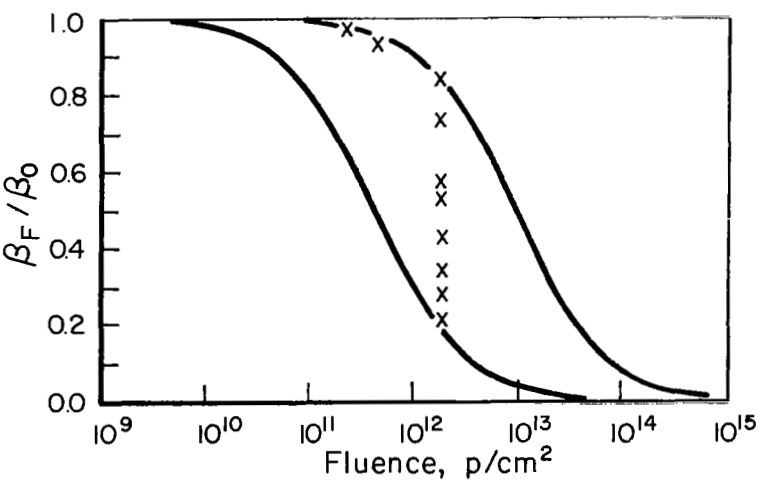

FIGURE 9. PROTON ENVIRONMENT LOW-LEVEL-SWITCHING APPLICATIONS, BIPOLAR TRANSISTOR BETA RATIO VERSUS FLUENCE

11 sets of data

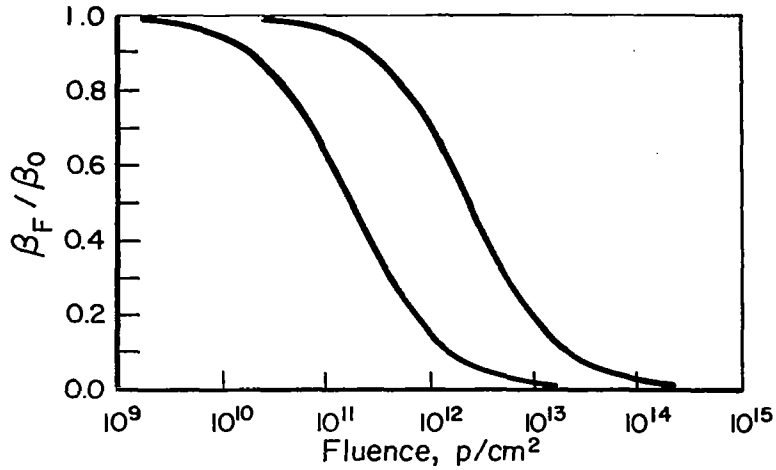

FIGURE 10. PROTON ENVIRONMENT HIGH-LEVEL-SWITCHING APPLICATIONS, BIPOLAR TRANSISTOR BETA RATIO VERSUS FLUENCE

26 sets of data

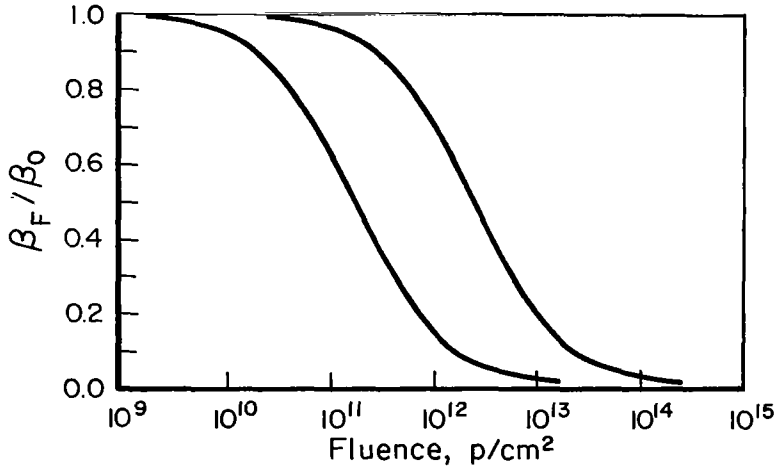

FIGURE 11. PROTON ENVIRONMENT POWER APPLICATIONS, BIPOLAR TRANSISTOR BETA RATIO VERSUS FLUENCE

26 sets of data

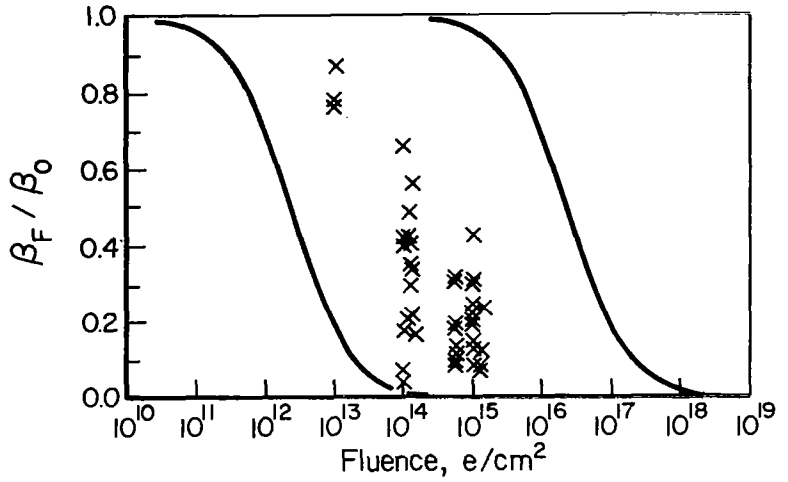

FIGURE 12. ELECTRON ENVIRONMENT AUDIO AND GENERAL PURPOSE APPLICATIONS, BIPOLAR TRANSISTOR BETA RATIO VERSUS FLUENCE

78 sets of data

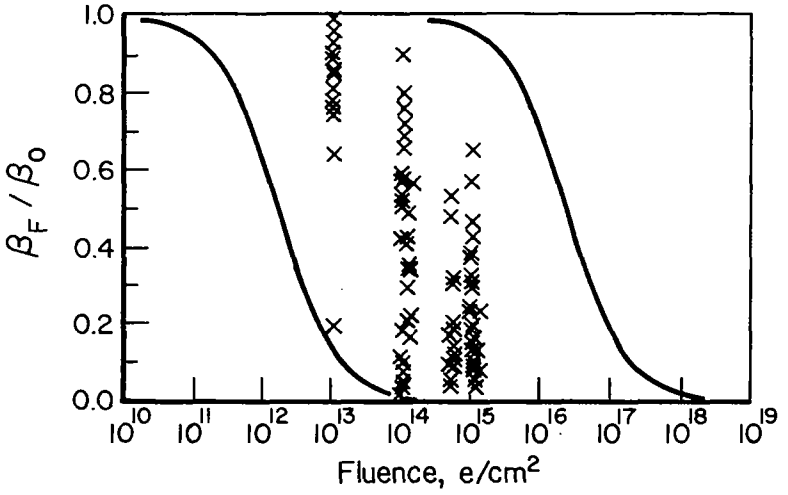

FIGURE 13. ELECTRON ENVIRONMENT HIGH-FREQUENCY APPLICATIONS, BIPOLAR TRANSISTOR BETA RATIO VERSUS FLUENCE

288 sets of data

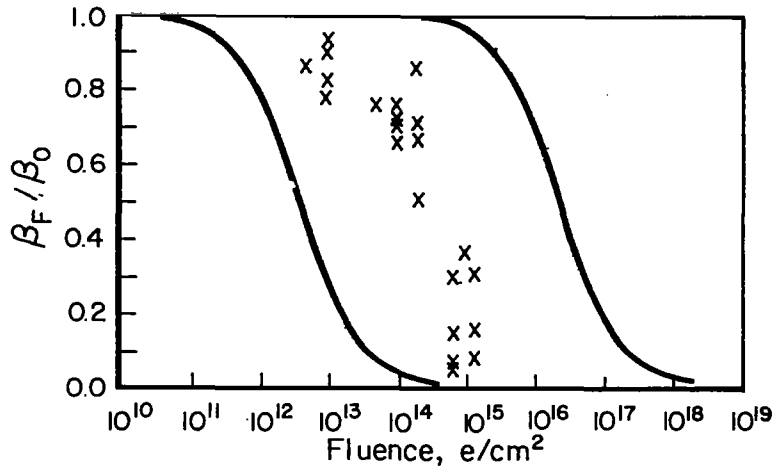

FIGURE 14. ELECTRON ENVIRONMENT LOW-LEVEL-SWITCHING APPLICATIONS, BIPOLAR TRANSISTOR BETA RATIO VERSUS FLUENCE

64 sets of data

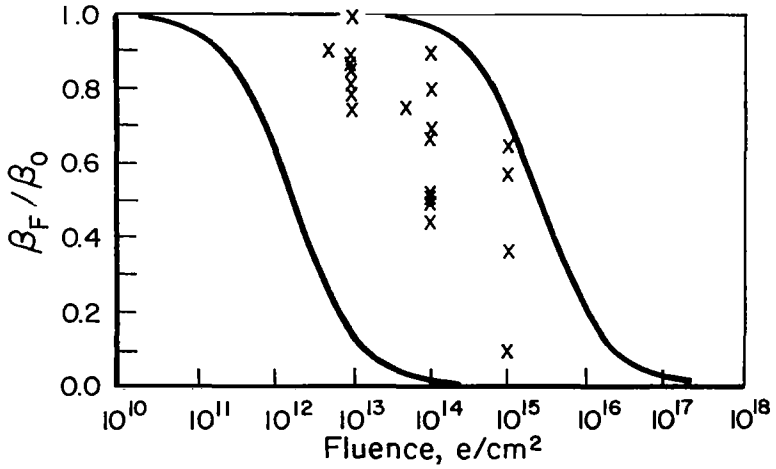

FIGURE 15. ELECTRON ENVIRONMENT HIGH-LEVEL-SWITCHING APPLICATIONS, BIPOLAR TRANSISTOR BETA RATIO VERSUS FLUENCE

146 sets of data

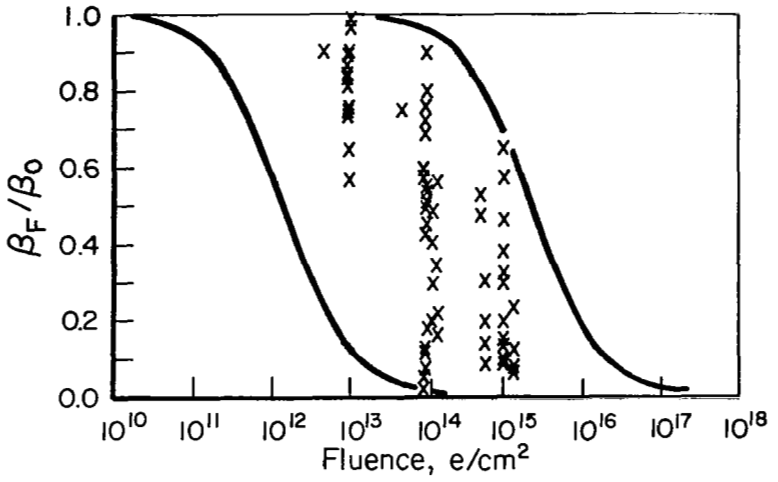

FIGURE 16. ELECTRON ENVIRONMENT POWER APPLICATIONS, BIPOLAR TRANSISTOR BETA RATIO VERSUS FLUENCE

167 sets of data

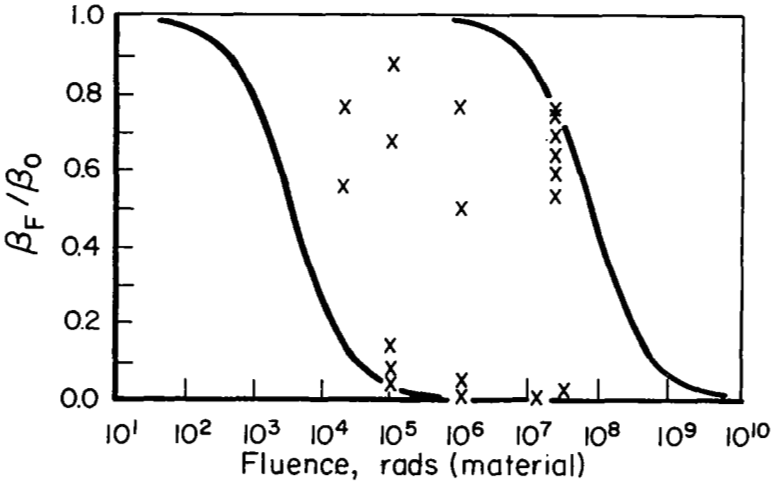

FIGURE 17. ELECTROMAGNETIC ENVIRONMENT AUDIO AND GENERAL PURPOSE APPLICATIONS, BIPOLAR TRANSISTOR BETA RATIO VERSUS FLUENCE

33 sets of data

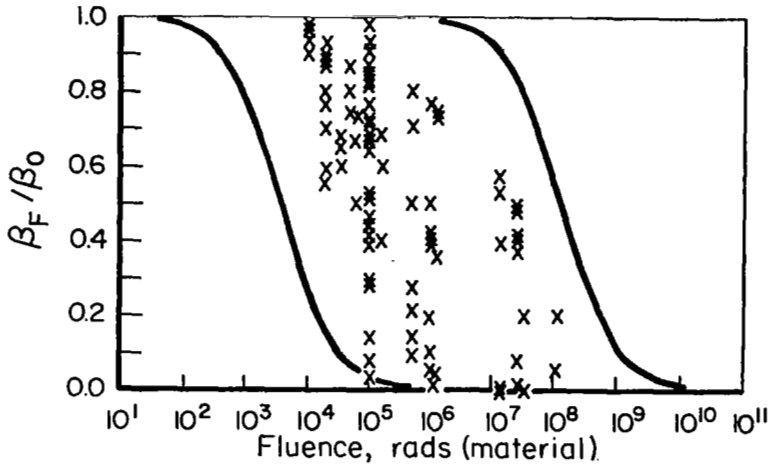

FIGURE 18. ELECTROMAGNETIC ENVIRONMENT HIGH-FREQUENCY APPLICATIONS, BIPOLAR TRANSISTOR BETA RATIO VERSUS FLUENCE

164 sets of data

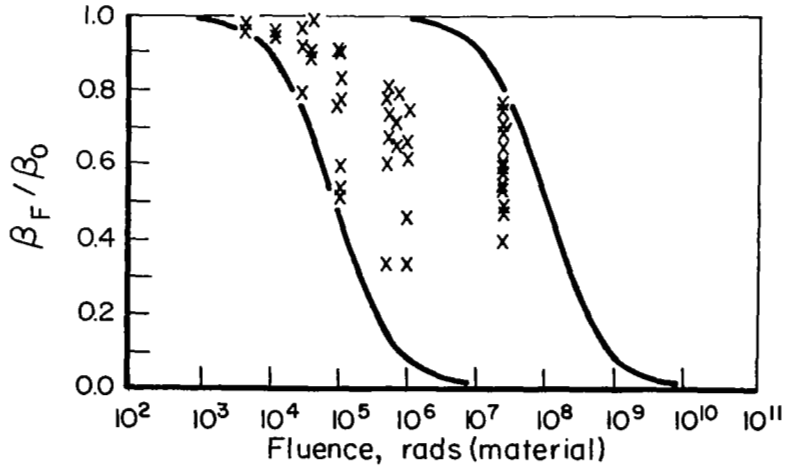

FIGURE 19. ELECTROMAGNETIC ENVIRONMENT LOW-LEVEL-SWITCHING APPLICATIONS, BIPOLAR TRANSISTOR BETA RATIO VERSUS FLUENCE

59 sets of data

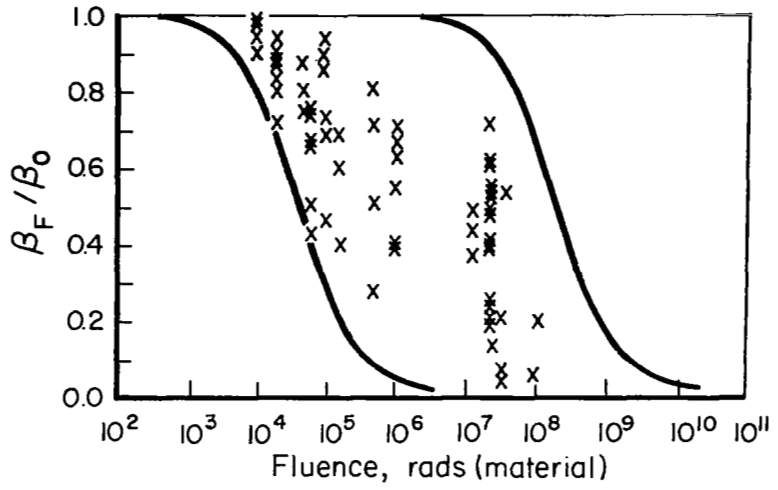

FIGURE 20. ELECTROMAGNETIC ENVIRONMENT HIGH-LEVEL-SWITCHING APPLICATIONS, BIPOLAR TRANSISTOR BETA RATIO VERSUS FLUENCE

106 sets of data

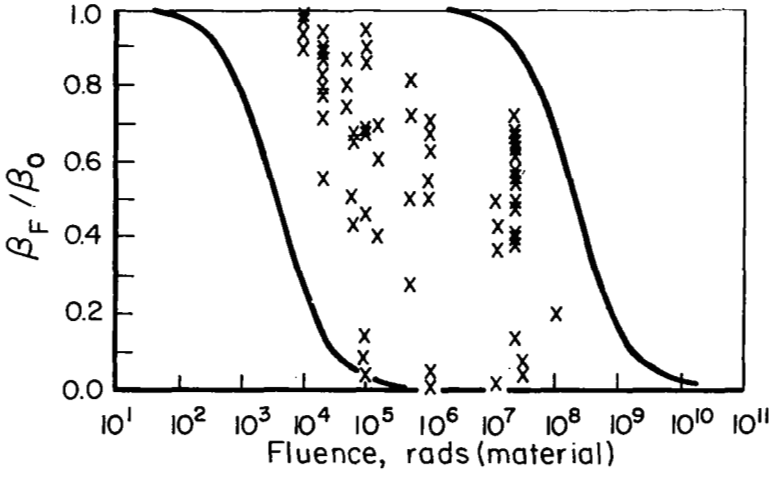

FIGURE 21. ELECTROMAGNETIC ENVIRONMENT POWER APPLICATIONS, BIPOLAR TRANSISTOR BETA RATIO VERSUS FLUENCE

120 sets of data

TABLE 1. RANGE AND MEDIAN VALUES OF BULK DAMAGE CONSTANT, K_b, FOR VARIOUS APPLICATION-ENVIRONMENT COMBINATIONS

Environment	Minimum K_b	Median K_b	Maximum K_b	Size of Data Base[a]
		Audio and General Purpose Applications		
Neutron	3.96×10^{-17} cm^2/n	3.38×10^{-16} cm^2/n	2.62×10^{-14} cm^2/n	21
Proton	5.08×10^{-17} cm^2/p	7.00×10^{-15} cm^2/p	1.11×10^{-14} cm^2/p	3
Electron	7.38×10^{-19} cm^2/e	1.72×10^{-16} cm^2/e	5.63×10^{-15} cm^2/e	78
Electromagnetic	2.43×10^{-10} rad^{-1}	1.43×10^{-9} rad^{-1}	1.92×10^{-9} rad^{-1}	33
		High-Frequency Applications		
Neutron	3.57×10^{-17} cm^2/n	4.52×10^{-16} cm^2/n	1.10×10^{-14} cm^2/n	131
Proton	6.24×10^{-16} cm^2/p	1.26×10^{-14} cm^2/p	2.38×10^{-13} cm^2/p	29
Electron	7.38×10^{-19} cm^2/e	3.71×10^{-17} cm^2/e	6.70×10^{-15} cm^2/e	288
Electromagnetic	5.85×10^{-11} rad^{-1}	8.10×10^{-9} rad^{-1}	1.92×10^{-6} rad^{-1}	164
		Low-Level-Switching Applications		
Neutron	1.52×10^{-17} cm^2/n	3.99×10^{-16} cm^2/n	2.56×10^{-14} cm^2/n	62
Proton	1.66×10^{-15} cm^2/p	5.72×10^{-15} cm^2/p	5.50×10^{-14} cm^2/p	11
Electron	7.38×10^{-19} cm^2/e	2.73×10^{-17} cm^2/e	1.28×10^{-15} cm^2/e	64
Electromagnetic	2.10×10^{-10} rad^{-1}	1.37×10^{-8} rad^{-1}	2.44×10^{-7} rad^{-1}	59
		High-Level-Switching Applications		
Neutron	1.15×10^{-16} cm^2/n	5.46×10^{-16} cm^2/n	4.60×10^{-14} cm^2/n	73
Proton	1.77×10^{-15} cm^2/p	1.29×10^{-14} cm^2/p	7.00×10^{-14} cm^2/p	26
Electron	2.22×10^{-18} cm^2/e	3.94×10^{-17} cm^2/e	5.00×10^{-15} cm^2/e	146
Electromagnetic	5.85×10^{-11} rad^{-1}	5.95×10^{-9} rad^{-1}	2.39×10^{-6} rad^{-1}	106
		Power Applications		
Neutron	5.25×10^{-17} cm^2/n	1.30×10^{-15} cm^2/n	1.21×10^{-13} cm^2/n	72
Proton	1.77×10^{-15} cm^2/p	1.29×10^{-14} cm^2/p	7.00×10^{-14} cm^2/p	26
Electron	4.27×10^{-18} cm^2/e	5.87×10^{-17} cm^2/e	6.70×10^{-15} cm^2/e	167
Electromagnetic	5.85×10^{-11} rad^{-1}	4.27×10^{-9} rad^{-1}	2.39×10^{-6} rad^{-1}	120

(a) The size of the data base gives the number of computed values of K_b used to determine the listed range and median values.

UNIJUNCTION TRANSISTORS

The unijunction transistor structure is shown schematically in Figure 22. Sometimes called a "double-base diode", this device displays a negative resistance characteristic which results from conductivity modulation of a moderately high resistivity silicon bar by means of injected minority carriers from the rectifying emitter contact. It is thus highly sensitive to radiation-induced changes in minority-carrier lifetime and resistivity.

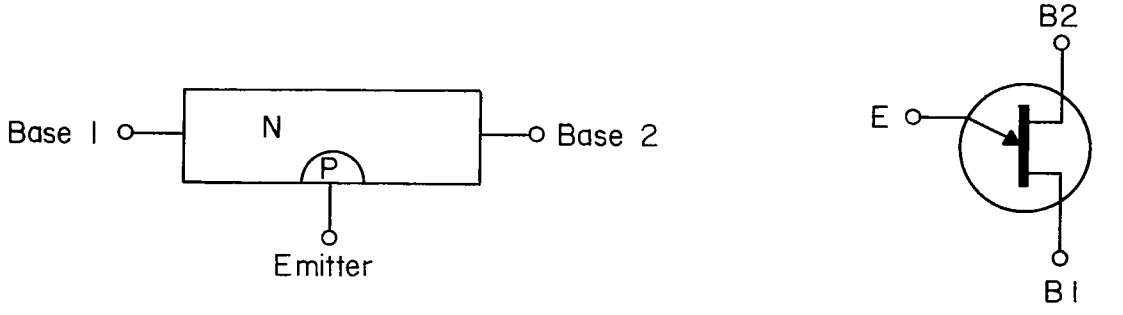

a. Unijunction Transistor Structural Diagram

b. Unijunction Transistor Schematic Symbol

FIGURE 22. STRUCTURAL DIAGRAM AND SCHEMATIC SYMBOL FOR UNIJUNCTION TRANSISTORS

The very limited amount of radiation-effects data that is available for unijunction transistors verifies that these devices have a very high sensitivity to radiation. The distance between the two ohmic base contacts is of the order of 5×10^{-2} cm. This corresponds to a bipolar transistor with an exceptionally wide base and results in the formation of an enormous number of trapping centers because of irradiation. The electrical effects of these trapping centers are further enhanced by the initially high silicon resistivity. Relatively low radiation fluences will significantly increase the resistivity of the N-type bar and change most of the properties of the device.* Ultimately most of the holes injected into the bar are captured.

The very significant changes observed in almost all of the important unijunction transistor parameters after relatively low radiation exposures

*Stanley, A. G., "Effect of Electron Irradiation on Electronic Devices", Technical Report 403, Massachusetts Institute of Technology, Lincoln Laboratory, November 3, 1965.

lead to the conclusion that the use of these devices in a radiation environment should be approached with caution. If their use is unavoidable, estimates of expected radiation effects can be made by comparison to the least radiation tolerant of the bipolar power transistors. Thus, adverse changes in the unijunction transistor parameters can be expected to be similar to the radiation-induced change in beta shown by the minimum envelope boundaries for power transistors in Figures 6, 11, 16, and 21.

FIELD-EFFECT TRANSISTORS

Field-effect transistors are unipolar devices which operate by electric-field control of majority-carrier conduction. The two basic types of field-effect transistors are the junction-field-effect transistor (JFET) and the insulated-gate-field-effect transistor (IGFET), discussed in the following paragraphs.

Junction-Field-Effect Transistors

A PN junction is the interface between channel and gate in a JFET. The structure is diagrammed and the schematic symbol shown in Figure 23 for both N-channel and P-channel JFET's. All JFET's operate in the depletion mode where a reverse bias, applied between gate and source, controls the current flow. Under these conditions a depletion region surrounds the channel of the JFET. The value of gate-to-source bias voltage (for zero or small drain-source voltage), for which the depletion region penetrates (from both sides) the entire thickness of the channel thus "pinching off" the current flow, is called the "pinch-off" voltage, V_p. With a zero gate-to-source bias voltage the current flow is a maximum.

For the N-channel JFET's, a negative gate voltage turns the device off, whereas for the P-channel JFET's a positive gate voltage is necessary to stop device conduction. FET's have a high input impedance relative to that of bipolar transistors and provide a voltage gain measured in terms of transconductance, G_m, similar to vacuum pentode tubes. A third important parameter is the total gate leakage current, I_{gss}, which is the current flowing from gate to channel for a zero drain-to-source potential. These three JFET parameters are the most sensitive to radiation damage.

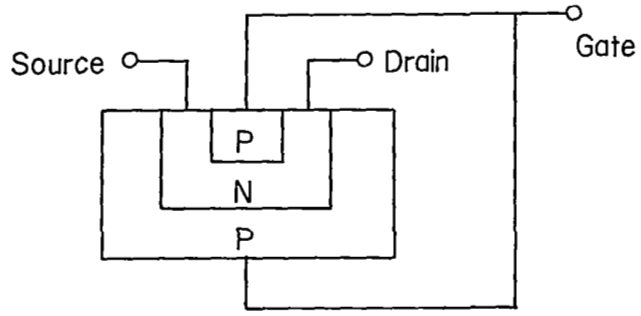

a. N-Channel JFET Structural Diagram

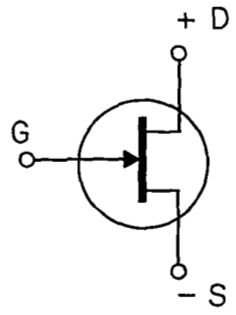

b. N-Channel JFET Schematic Symbol

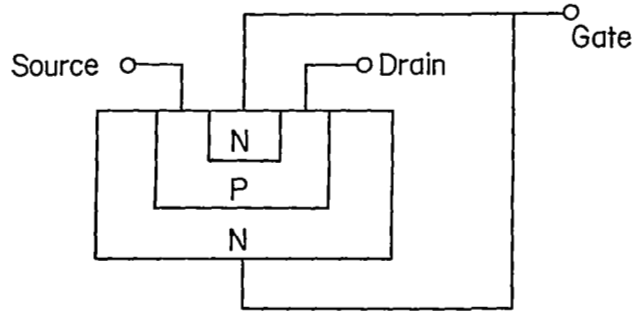

c. P-Channel JFET Structural Diagram

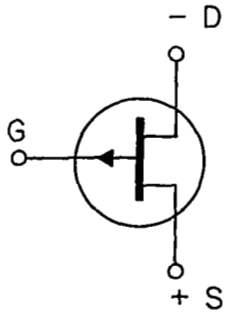

d. P-Channel JFET Schematic Symbol

FIGURE 23. STRUCTURAL DIAGRAMS AND SCHEMATIC SYMBOLS FOR N- AND P-CHANNEL JUNCTION-FIELD-EFFECT TRANSISTORS

The general effects of radiation on JFET's can be summarized as follows:

(1) The transconductance, G_m, and the "pinch-off" voltage, V_p, will decrease because of a radiation-induced change in effective impurity concentration that increases channel resistivity and changes carrier mobility.

(2) Increases in leakage current, I_{gss}, will be observed as a result of radiation-induced carrier generation surface contaminants near the junction edge and recombination-generation in the depletion region due to the introduction of recombination levels deep in the energy gap.

Representative values* for the ratio of postirradiation to preirradiation transconductance, $G_m(F)/G_m(0)$, are plotted versus fluence for P-channel JFET's in Figures 24 and 25 in the neutron and the electromagnetic environment, respectively. Available information is too limited to permit similar plots for other radiation environments or for N-channel JFET's. However, based on observations for a very few part types it appears that significant radiation-induced decreases in JFET G_m would not be expected for fluences less than 10^{11} n/cm^2, or 10^{15} e/cm^2, or 10^5 rads (Si) of electromagnetic radiation. No proton data for JFET's are available. Of course, specific device types may have superior radiation tolerance but the information presently available permits only these generalizations.

The data available showing the effects of radiation on V_p for JFET's are too limited to permit the presentation of trend plots. However, it appears that the fluences producing significant reductions in the value of this parameter are at least as large as those producing significant reductions in G_m.

The significance of radiation-induced increases in I_{gss} depends upon the circuit usage. Where signal levels are high, increased values of I_{gss} can often be tolerated without degrading circuit performance. In low-level circuits small values of leakage current can be detrimental.

The information available about radiation-induced leakage currents in JFET's also is very limited. Figure 26 shows available values for the ratio of postirradiation to preirradiation P-channel JFET leakage current, $I_{gss}(F)/I_{gss}(0)$, plotted versus neutron fluence. These data are for a single

*The values plotted fo the neutron environment are representative of 28 sets of data available for four device types. For the elect magnetic environment the plotted values represent 143 sets of data available for six device types.

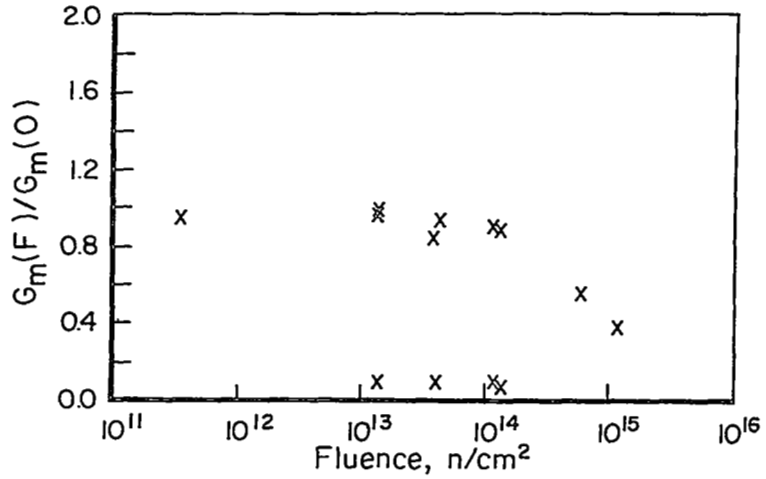

FIGURE 24. NEUTRON ENVIRONMENT, P-CHANNEL JUNCTION-FIELD-EFFECT TRANSISTOR, RADIATION EFFECT ON TRANSCONDUCTANCE

28 sets of data

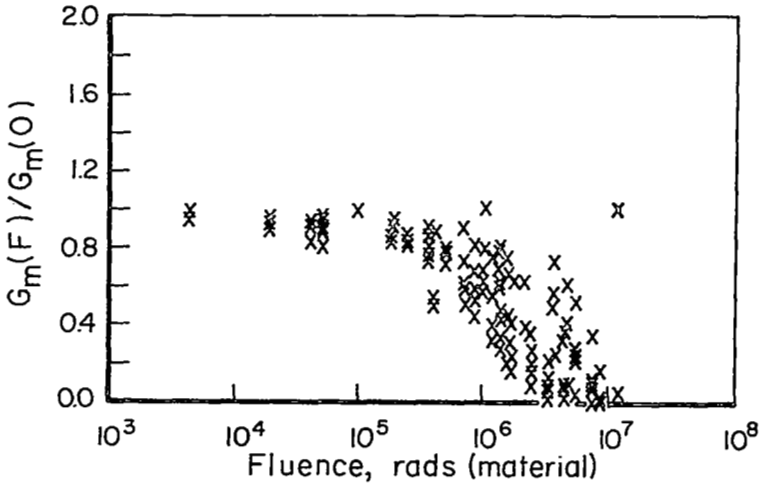

FIGURE 25. ELECTROMAGNETIC ENVIRONMENT, P-CHANNEL JUNCTION-FIELD-EFFECT TRANSISTOR, RADIATION EFFECT ON TRANSCONDUCTANCE

143 sets of data

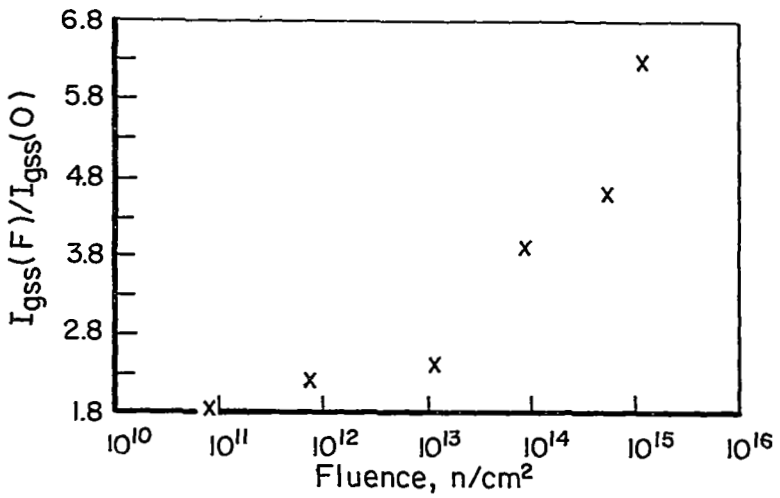

FIGURE 26. NEUTRON ENVIRONMENT, P-CHANNEL JUNCTION-FIELD-EFFECT TRANSISTOR, RADIATION EFFECT ON LEAKAGE CURRENT

6 sets of data

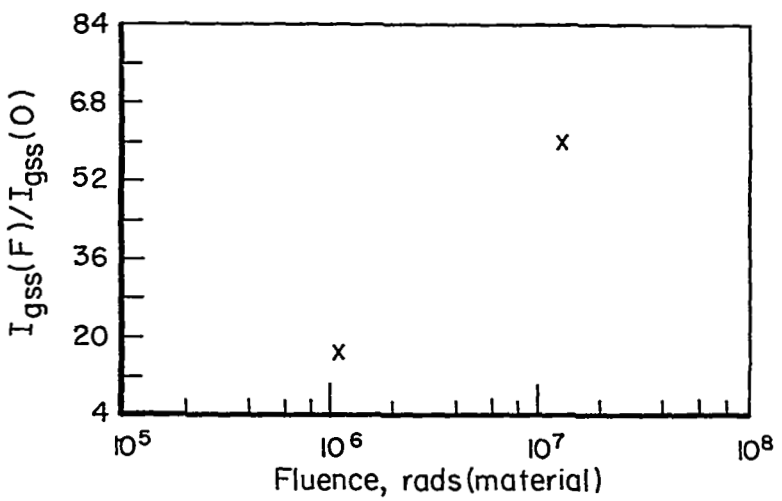

FIGURE 27. ELECTROMAGNETIC ENVIRONMENT, N-CHANNEL JUNCTION-FIELD-EFFECT TRANSISTOR, RADIATION EFFECT ON LEAKAGE CURRENT

3 sets of data

part type, the TIX693. The $I_{gss}(F)/I_{gss}(0)$ data available for a 2N3089A N-channel JFET at three electromagnetic fluences are plotted in Figure 27. Generalizations about the fluences for which radiation-induced leakage currents become significant cannot be made until additional experimental data on other part types becomes available and unless usage is known.

Insulated-Gate-Field-Effect Transistors

The IGFET has a dielectric layer that insulates the channel from the gate. There are several dielectric materials used for this layer, but the most common is silicon dioxide (SiO_2). An IGFET using SiO_2 as dielectric is normally called a metal-oxide-semiconductor field-effect transistor (MOSFET).

Thin-film field-effect transistors (TFT's) constitute another important category of IGFET's. The TFT's employ geometrically controlled surface films on a polycrystalline substrate. Typical semiconductor films employed are: cadmium selenide (CdSe), cadmium sulfide (CdS), or epitaxially deposited silicon, while the substrate material is usually glass, ceramic, or sapphire.

Metal-Oxide-Semiconductor Field-Effect Transistors

MOSFET's are constructed to operate in one or both of the depletion or enhancement modes. In the depletion mode a reverse bias applied between gate and source produces a depletion region surrounding the channel thereby reducing the current flow. As for the JFET's the bias for which the current cuts off completely, is called "pinch-off" voltage, V_p. With zero gate voltage, the current flow is heavy. The structural diagrams and schematic symbols for depletion mode MOSFET's are shown in Figure 28.

In the enhancement-mode MOSFET, the application of reverse bias between gate and source induces a channel, increasing or "enhancing" the current flow. With zero gate voltage, the source to drain structure looks like two PN junctions back to back and there is no current flow. The structural diagrams and schematic symbols for enhancement MOSFET's are shown in Figure 29. Some MOSFET types are constructed for operation in either the depletion mode or in the enhancement mode.

Transconductance, G_m, gate leakage current, I_{gss}; and "pinch-off" voltage, V_p, are important parameters for depletion mode MOSFET's as

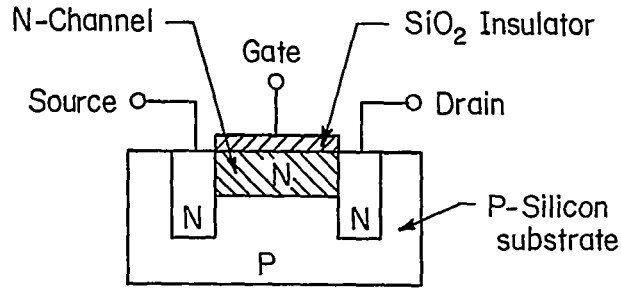

a. N-Channel Depletion MOSFET
Structural Diagram

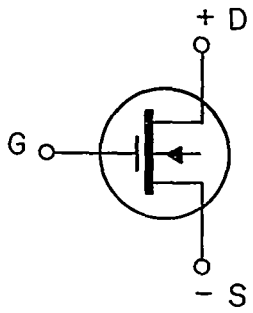

b. N-Channel Depletion MOSFET
Schematic Symbol

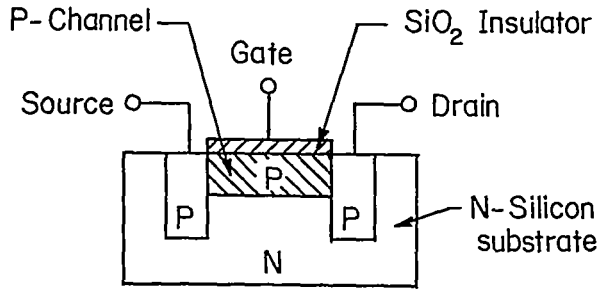

c. P-Channel Depletion MOSFET
Structural Diagram

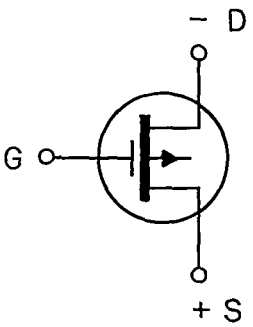

d. P-Channel Depletion MOSFET
Schematic Symbol

FIGURE 28. STRUCTURAL DIAGRAMS AND SCHEMATIC SYMBOLS FOR N- AND P-CHANNEL DEPLETION METAL-OXIDE-SEMICONDUCTOR FIELD-EFFECT TRANSISTORS

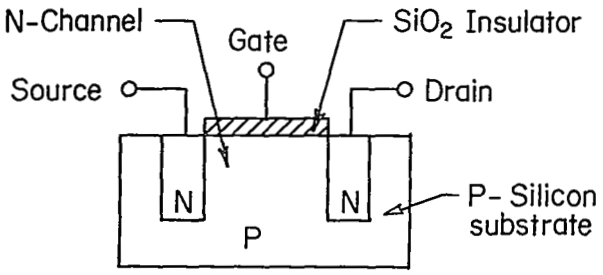

a. N-Channel Enhancement MOSFET Structural Diagram

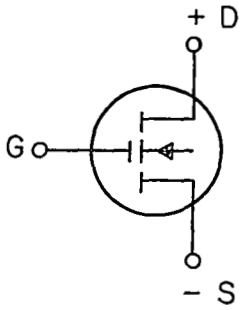

b. N-Channel Enhancement MOSFET Schematic Symbol

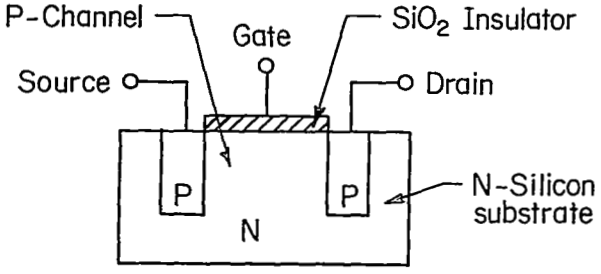

c. P-Channel Enhancement MOSFET Structural Diagram

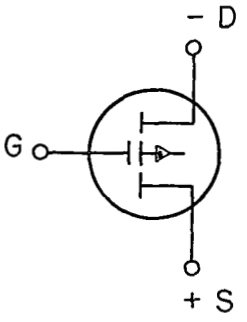

d. P-Channel Enhancement MOSFET Schematic Symbol

FIGURE 29. STRUCTURAL DIAGRAMS AND SCHEMATIC SYMBOLS FOR N- AND P-CHANNEL ENHANCEMENT METAL-OXIDE-SEMICONDUCTOR FIELD-EFFECT TRANSISTORS

they are for JFET's. For the enhancement mode MOSFET's, the important voltage parameter is the threshold voltage, V_{gth}, which is the voltage from gate to source required to enhance the channel and thus increase current flow. The important leakage current for enhancement mode MOSFET's is the drain to substrate leakage current, I_{dss}.

The general effects of radiation on MOSFET's can be summarized as follows:

(1) The threshold voltage, V_{gth}, will increase because radiation induces (by ionization) a buildup of a positive charge in the SiO_2 layer that is semipermanent (months). These changes in V_{gth} affect most of the other MOSFET parameters.

(2) Increases in the leakage currents, I_{gss} or I_{dss}, are observed as the result of carrier generation-recombination in the depletion region and surface contaminants near the junction edge.

(3) Changes in channel resistivity and carrier mobility result from radiation-induced changes in the effective impurity concentration causing decreases in V_p and G_m.

Damage in MOSFET's is caused primarily by ionizing radiation. The most radiation-sensitive MOSFET parameter is the threshold voltage, V_{gth}, for enhancement mode devices, or the "pinch-off" voltage, V_p, for depletion-mode devices. In general, degradation of V_{gth} or V_p proceeds rapidly in the range of 10^3 to 10^4 R, but becomes more gradual above this exposure. Complete failure, i.e., zero transconductance, has been observed at exposures of 10^6 to 10^7 R.

As previously stated, changes in V_{gth} in MOSFET's result from radiation-induced surface charge at the Si-SiO_2 interface. These voltage changes caused by the charge buildup have the same effect as voltage applied directly to the gate; e.g., the current-voltage curves for MOSFET's approximately retain their shape but are translated to more negative gate biases with radiation. Because of rapid recombination in the silicon region, no permanent changes result from charges generated in the silicon. However, in silicon dioxide the radiation-generated holes are relatively immobile and are trapped or recombined before they leave the oxide. The electrons are mobile and thus drift toward the positive electrode where they are removed

from the oxide. Since electrons cannot enter the oxide from the silicon because of the potential barrier at the Si-SiO_2 interface, a positive charge builds up near the interface. The charge increases and then saturates with increasing dose. The saturation value of the positive charge depends on the gate potential.*

The exact dependence of the saturated value of radiation-induced charge on the gate bias is determined by the distribution of the charges in the oxide. Normally, a nearly linear dependence of charge-saturation value on gate voltage is observed over a range of several volts. The charge buildup appears to be independent of oxide thickness, indicating a dependence on gate voltage but not on the applied field. The charge buildup is independent of the dose rate at least for positive gate voltages.** Some dose-rate dependence of the charge buildup has been observed for zero and negative gate voltage.*

Available information showing the effects of radiation on MOSFET's is limited to a few measurements of a few part types. The values available for $G_m(F)/G_m(0)$ and $V_{gth}(F)/V_{gth}(0)$ are listed together with the fluence in Table 2. Representative values of $V_{gth}(F)/V_{gth}(0)$ selected from 22 measurements for the two types of P-channel enhancement MOSFET's are plotted versus 1.5 MeV electron fluence in Figure 30. No leakage current data are available at this time.

Other Insulated-Gate-Field-Effect Transistors

Metal-insulator-semiconductor field-effect transistors (MISFET's) are IGFET structures that have a material other than silicon dioxide as a gate insulator. Metal-nitride-silicon (MNS) and metal-nitride-oxide-silicon (MNOS) structures exemplify this class of devices. These devices are of particular interest where a high radiation flux exists in the use environment since laboratory prototype devices indicate an improved radiation tolerance to flux dependent effects. No specific information is available for commercial MISFET devices at high radiation fluences but it is reasonable to expect a performance comparable to that of MOSFET devices.

*Mitchell, J. P., "Radiation-Induced Space-Charge Buildup in MOS Structures", IEEE Transactions on Electron Devices, ED-14, November, 1967, p.774.

**Snow, E. H., et al., "Radiation Study on MOS Structures", Fairchild Semiconductor, Contract AF 19(628)-5747, January, 1967.

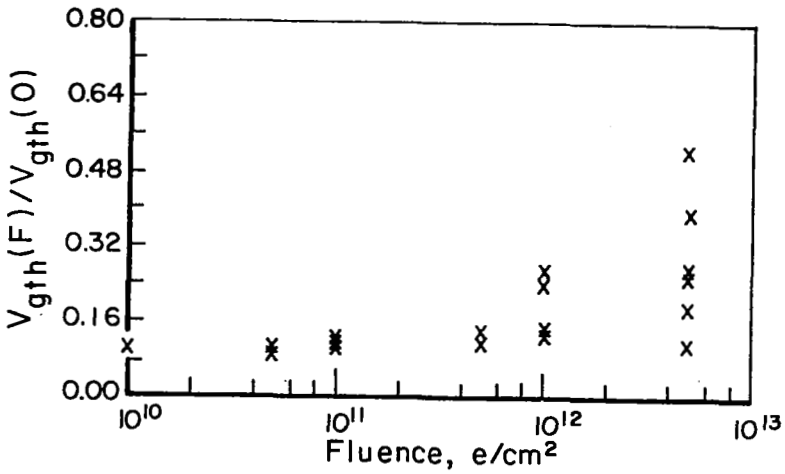

FIGURE 30. ELECTRON ENVIRONMENT, P-CHANNEL MOS FIELD-EFFECT TRANSISTOR, RADIATION-EFFECT ON GATE THRESHOLD VOLTAGE

Twenty-two sets of data.

Thin-Film Transistors

As previously stated TFT's consist essentially of an FET structure deposited on a polycrystalline substrate. Various combinations of semiconductor films, gate insulating materials and substrate materials may be used. Most of the small amount of available radiation-effects information for TFT's is for developmental devices and its applicability to production types is questionable. In general, it appears that TFT's can be expected to respond to radiation similarly to MOSFET's. Estimation of fluence levels causing significant parameter changes does not appear warranted at this time.

TABLE 2. RADIATION EFFECTS ON MOSFET PARAMETERS

Type	Channel Type	Operating Mode	$G_m(F)/G_m(0)$	$V_{gth}(F)/V_{gth}(0)$	Fluence
TA 2330	N	Enhancement	0.13	--	5×10^{14} n/cm^2 (E > 10 keV)
TA 2330	N	Enhancement	0.33	--	5×10^{14} n/cm^2 (E > 10 keV)
TA 2330	N	Enhancement	--	0.52	5×10^{14} n/cm^2 (E > 10 keV)
FN 1002	P	Enhancement	0.71	0.47	5×10^{14} n/cm^2 (E > 10 keV)
X 1004GME	P	Enhancement	0.36	0.15	5×10^{14} n/cm^2 (E > 10 keV)
X 1004GME	P	Enhancement	0.70	--	5×10^{14} n/cm^2 (E > 10 keV)
X 1004GME	P	Enhancement	1.00	--	5×10^{5} rads (Si) (Co^{60})
2N3608	P	Enhancement	--	1.01	2×10^{10} p/cm^2 (E = 100 MeV)
2N3608	P	Enhancement	--	1.34	8×10^{11} p/cm^2 (E = 140 MeV)
FI 100	P	Enhancement	0.81 - 0.91	--	5×10^{12} e/cm^2 (E = 1.5 MeV)
FI 100[a]	P	Enhancement	--	1.0 - 2.48	1×10^{10} - 5×10^{12} e/cm^2 (E = 1.5 MeV)
MM 2103[a]	P	Enhancement	0.89 - 0.96	--	5×10^{12} e/cm^2 (E = 1.5 MeV)
MM 2103[a]	P	Enhancement	--	0.95 - 5.25	1×10^{10} - 5×10^{12} e/cm^2 (E = 1.5 MeV)

(a) See Figure 30.

BIBLIOGRAPHY

Anspaugh, B. E., "High Energy Proton Testing of Mariner IV Components", California Institute of Technology, Jet Propulsion Laboratories, Pasadena, California, JPL-TM-33-314, Tech. Memo, NAS7-100, January 1, 1967.

Brown, R. R., The Boeing Company, Seattle, Washington, "Equivalence of Radiation Particles for Permanent Damage in Semiconductor Devices", IEEE Transactions on Nuclear Science, NS-10 (5), November, 1963, pp 54-57.

Brucker, G., Dennehy, W., and Holmes-Siedle, A., Radio Corporation of America, Astroelectronic Division, Princeton, New Jersey, "High-Energy Radiation Damage in Silicon Transistors", paper presented at the IEEE Annual Conference on Nuclear and Space Radiation Effects, Ann Arbor, Michigan, July 12-15, 1965.

Garrett, C.G.B., and Brattain, W. H., "Some Experiments on, and a Theory of, Surface Breakdown", Journal of Applied Physics, 27, 1956, p 299.

Gordon, F., Jr., and Wannemacher, H. E., Jr., "The Effects of Space Radiation on MOSFET Devices and Some Application Implications of Those Effects", NASA, Goddard Space Flight Center, Greenbelt, Maryland, X-716-66-347, August, 1966.

Hofstein, S. R., and Heiman, F. P., "The Silicon Insulated-Gate Field-Effect Transistor", Procceedings of the IRE, 51, 1963, p 1190.

Holmes-Siedle, A. G., Radio Corporation of America, Princeton, New Jersey, "Space Radiation: Its Influence on Satellite Design", RCA Engineering, 11, June-July, 1965, pp 8-14.

Hughes, H. L., and Giroux, R. R., Naval Research Laboratory, Washington, D. C., "Space Radiation Effects MOSFET's, Electronics, 37 (32), December 28, 1964.

Kaufman, A. B., Newhoff, H. R., and Gaz, R. A., "Effects of Neutron and Gamma Ray Spectra on Flight Control Systems", Litton Systems, Inc., Woodland Hills, California, FDL-TDR-64-30, Feburary, 1964, Tech. Doc. Rpt., January, 1963 - March, 1964, AF 33(657)-10584.

Lockheed Aircraft Corporation, "Components Irradiation Test No. 19 Gamma Irradiation of 2N914, 2N198, S2N930, 2N2192, and 2N2369 Transistors", Lockheed Georgia Company, Marietta, Georgia, ER-8623, NASA-CR-82010, October, 1966. Avail: NASA, N67-18545.

Measel, P. R., and Brown, R. R., The Boeing Company, Seattle, Washington, "Low Dose Ionization-Induced Failures in Active Bipolar Transistors", paper presented at the IEEE Conference on Nuclear and Space Radiation Effects, Missoula, Montana, July 15-18, 1968.

Nelson, D. L., Sweet, R. J., and Niehaus, D. J., "Study to Investigate the Effects of Ionizing Radiation on Transistor Surfaces", The Bendix Corporation, Southfield, Michigan, Bendix-R-3699, January, 1967, Final Report, NAS 8-20135.

Peletier, D. P., "The Effects of Ionizing Radiation on Transistors", The Johns Hopkins University, Applied Physics Laboratory, Silver Springs, Maryland, TG-937, August, 1967, Tech. Memo., NOw-62-0604-c. Avail: DDC, AD 659295.

Radio Corporation of America, "TOS Radiation Program Report. Analysis and Evaluation of Test Results", Astro-Electronics Division, Princeton, New Jersey, September, 1965.

Radio Corporation of America, "TOS Radiation Test. Series No. 2 (February, 1965)", Astro-Electronics Division, Princeton, New Jersey, Engineering Report, September, 1965.

Raymond, J., Steele, E., and Chang, W., Northrop Corporation, Ventura Division, Newbury Park, California, "Radiation Effects in Metal-Oxide-Semiconductor Transistors", IEEE Transactions of Nuclear Science, NS-12 (1), February, 1965, 11th Nuclear Science Symposium Instrumentation in Space and Laboratory, Philadelphia, Pennsylvania, October 28-30, 1964, pp 457-463.

Rind, E., and Bryant, F. R., NASA, Langley Research Center, Instrument Research Division, Hampton, Virginia, "Experimental Investigation of Simulated Space Particulate Radiation Effects on Microelectronics", paper presented at the Conference on Nuclear Radiation Effects, jointly sponsored by the Institute of Electrical and Electronics Engineers, the Professional and Technical Group on Nuclear Science, and the University of Washington, Seattle, Washington, July 20-23, 1964.

Roberts, C. S., and Hoerni, J. A., "Comparative Effects of 1 MeV Electron Irradiation on Field Effect and Injection Transistors", Teledyne, Inc., Amelco Semiconductor Division, Mountain View, California, Tech. Bul. No. 1, March, 1963, Field Effect Transistors Tech. Bulletin.

Robinson, M. N., Kimble, S. G., and Walker, D. M., "Low Flux Nuclear Radiation Effects on Electrical and Electronic Components (BMI-LF-3)", North American Aviation, Inc., Atomics International Division, Canoga Park, California, NAA-SR-9634, December 1, 1964, AT-(11-1)-Gen-8. Avail: NASA, N65-12642.

Sah, C. T., "A New Semiconductor Tetrode – The Surface Potential Controlled Transistor", Proceedings of the IRE, 51, 1963, p 119.

Wannemacher, H. E., "Gamma, Electron, and Proton Radiation Exposures of P-Channel, Enhancement, Metal Oxide Semiconductor, Field Effect Transistors", NASA, Goddard Space Flight Center, Greenbelt, Maryland, X-716-65-351, August, 1965.

Index

NASA-Langley, 1971 — 9 CR-1834